Structure and Physical Properties of Syndiotactic Polypropylene from Living Polymerization with Bis(phenoxyimine)-Based Titanium Catalysts

Claudio De Rosa,*,† Teresa Circelli,† Finizia Auriemma,† Robert T. Mathers,‡ and Geoffrey W. Coates‡

Dipartimento di Chimica, Università degli studi di Napoli "Federico II", Complesso Monte S. Angelo, Via Cintia, 80126 Napoli, Italy, and Department of Chemistry and Chemical Biology, Baker Laboratory, Cornell University, Ithaca, New York 14853-1301

Received June 23, 2004; Revised Manuscript Received September 1, 2004

ABSTRACT: A study of the structure and mechanical properties of syndiotactic polypropylene prepared with non-metallocene catalysts, based on titanium chlorides bearing phenoxyimine ligands, is reported. This catalyst promotes living polymerization of propylene, producing high molecular weight syndiotactic polypropylene, through a secondary (2,1) mechanism of enchainment of monomer and chain-end control of stereoselectivity. The effect of the presence of *m* dyads defects of stereoregularity, consistent with the chain-end mechanism, and defects of regioregularity, due to (1,2) misinsertions, on the crystallization behavior and mechanical properties is analyzed. As-prepared samples crystallize in conformationally disordered modifications of the isochiral helical form II containing kink-bands defects. This is probably due to the presence of regiodefects, producing pairs of vicinal methylene groups along the polymer chains, which favors, locally, the formation of trans-planar sequences that, in turn, induces the crystallization of the sample in the kink-bands disordered modification of form II. This also explains the observed stability of the trans-planar form III obtained in stretched fibers, which does not transform completely in helical forms by releasing the tension or by annealing, as instead occurs in metallocene-made syndiotactic polypropylene. The kink-bands disordered modifications are metastable and transform into the most stable antichiral helical form I by crystallization from the melt. However, disordered modifications of form I are obtained, even at high crystallization temperatures. The presence of *m* dyads defects of stereoregularity prevents the crystallization of the fully ordered antichiral helical form I. These defects may induce inversions of the helical chirality along the chains so that correlations at long distances between the chirality of the helices along *a* and *b* axes of the unit cell are destroyed. The particular microstructure also influences the mechanical properties. The analyzed sample presents values of elastic modulus lower than that of metallocene-made syndiotactic polypropylene of similar stereoregularity, due to higher flexibility of chains and the presence of higher degrees of disorder in crystals induced by the microstructural defects. Unoriented compression-molded samples show a remarkable elastic recovery even though the sample is crystalline and experiences plastic deformation during stretching. As a consequence, oriented fibers present good elastic properties in a large deformation range. The elasticity is associated with polymorphic transitions occurring in the crystals during the mechanical stress−relaxation cycles.

Introduction

Syndiotactic polypropylene (s-PP) was synthesized for the first time in the 1960s by Natta and Zambelli using a series of homogeneous vanadium-based catalysts at low temperature.[1] The propylene monomer was enchained with secondary (2,1) regiochemistry, and stereocontrol was derived from a chain-end mechanism.[2−4] Because of the poor syndiospecificity and regiospecificity of the vanadium-based catalysts, the resulting polymer had scarcely interesting physicochemical properties and has received in the past only very little attention.

The mechanism of secondary insertion of monomer is not common with Ziegler−Natta and metallocene catalysts. The polymerization reactions are generally agreed to proceed by coordination of the olefin to a metal, followed by migratory insertion of the coordinated olefin into the growing polymer chain. For heterogeneous Ziegler−Natta catalysts as well as metallocenes, α-olefin insertions into metal−alkyl bonds occur predominately with primary (1,2) regiochemistry, where the methylene carbon atom is bound to the metal. Small amounts of regioerrors (<1%) are, however, observed in polypropylenes prepared with isospecific metallocene catalysts.[5] In these cases (2,1)-insertions generally lower catalyst activity and molecular weights of the polymers because insertion rates of olefin into the more bulky secondary metal−alkyl species are slowed, and β-hydride elimination and chain-end isomerization (1,3-insertion) become more competitive with chain growth.[6]

It has also been shown that few catalysts produce higher levels of secondary insertion, as the zirconocene *rac*-$C_2H_4(4,7\text{-}Me_2H_4Ind)_2ZrCl_2$ (Me = methyl, Ind = indenyl) activated with methylalumoxane (MAO) reported by Spaleck,[7,8] which gives about 19% regioinversion, or the sulfur-bridged bis(phenolate)titanium catalyst of Kakugo,[9] which produces nearly completely regioirregular polypropylenes. Moreover, Brookhart[10] and Gibson[11] have reported iron-based catalysts that produce moderately isotactic polypropylene through a secondary insertion and a chain-end control mechanism.[12−14]

These examples indicate that both exclusive secondary regiochemistry and chain-end stereocontrol mech-

† Università degli studi di Napoli "Federico II".
‡ Cornell University.
* To whom correspondence should be addressed: Tel ++39 081 674346; Fax ++39 081 674090; e-mail claudio.derosa@unina.it, derosa@chemistry.unina.it.

10.1021/ma048753j CCC: $27.50
Published on Web 10/28/2004

Chart 1. Catalyst Precursors Based on Bis(phenoxyimine)titanium Complex for the Living Polymerization of Propylene to Highly Syndiotactic Polypropylene[20−22]

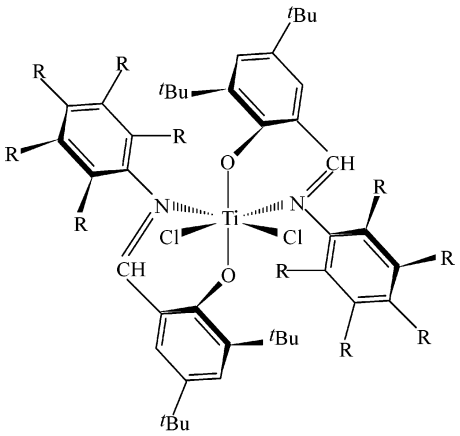

1. R = H
2. R = F

anism have not been obtained with metallocene or Ziegler−Natta catalytic systems.

Remarkable degrees of chain-end control have been observed for various C_{2v}-symmetric catalyst precursors. For instance, the Cp_2TiPh_2/MAO catalyst system (Cp = cyclopentadienyl, Ph = phenyl) of Ewen produces poorly isotactic polypropylene at low temperatures,[15] but chain-end stereocontrol is completely lost at elevated temperatures, giving an atactic polymer. Also in the case of a syndiospecific polymerization of propylene, besides the vanadium-based catalyst of Natta and Zambelli,[1] high degrees of chain-end control have been observed by Pellecchia with nickel-based MAO-activated complex at −78 °C.[16] The polymerization proceeds by a primary insertion mechanism, as in metallocene systems,[17−19] but also in this case the stereocontrol is lost at ambient temperatures, producing an atactic polymer.

An example of catalytic system able to produce stereoregular polymers through a chain-end mechanism even at ambient temperature is the iron-based complex bearing bis(imino)pyridyl ligands, reported by Brookhart.[14] This catalyst produces relatively high degrees of isotacticity at −20 °C and moderately isotactic-enriched polymers even at 20 °C[13] due to the secondary (2,1)-insertion mechanism.

Only recently, Coates et al. have found a new family of nonmetallocene catalysts based on titanium chlorides bearing phenoxyimine (PHI) ligands (Chart 1), which are able to promote living polymerization of propylene producing highly syndiotactic polypropylene with high molecular weight,[20] through exclusive chain-end control of stereoregularity and secondary (2,1) mechanism of monomer enchainment. These catalysts also produce ethylene and propylene-based block copolymers[21,22] and are based on a class of compounds extensively studied by Mitsui for ethylene polymerization.[23−28] It is worth noting that at variance with the chiral C_2-symmetric metallocenes discovered by Ewen[15] and Brintzinger and Kaminsky,[29] which produce isotactic polymers, the C_2-symmetric nonmetallocene catalysts of Chart 1 produce highly syndiotactic polypropylenes.[20,21] Coates et al.[20−22] have proposed that the selectivity was derived from chain-end control enhanced by a secondary mechanism of enchainment. Fujita and co-workers have recently reported evidences of the presence of end groups of polypropylenes consistent with elimination following 2,1-insertion of propylene.[30] Moreover, end group analysis revealed that insertion of propylene into the initiating titanium hydride occurs with high 1,2-regiochemistry. Subsequent insertions into primary titanium alkyls are regiorandom, while insertions into secondary titanium alkyls proceed with high 2,1-regioselectivity.[22]

Because of the chain-end stereocontrol and the secondary (2,1) insertion, s-PP prepared with phenoxyimine-based titanium catalysts of Chart 1 presents a microstructure different from that of s-PP prepared with C_s-symmetric metallocene catalysts.[31] Chains of s-PP prepared with nonmetallocene catalysts of Chart 1 are, indeed, characterized by defects of stereoregularity represented basically by isolated *m* dyads (*..rrrmrrr..*), consistent with chain-end control, and pairs of vicinal methylene groups as a result of occurrence of defects in the secondary (2,1)-regiospecificity. Samples prepared with C_s-symmetric metallocene catalysts are instead characterized by *mm* triads stereodefects,[31] whose amount depends on the polymerization temperature, consistent with the enantiomorphic site control mechanism, and *m* dyads defects as a results of skipped insertion.

In the past years we have shown that the crystallization and the physical properties of isotactic and syndiotactic polypropylenes prepared with metallocene catalysts strongly depend on the microstructure of the polymer chains, in particular on the kind of stereo- and regiodefects and on the distribution of defects along the polymer chains.[32−40] It is, therefore, expected that the different types of defects present in chains of s-PP samples prepared with the nonmetallocene phenoxyimine-based catalysts (Chart 1) may induce different crystallization and physical properties in the resulting materials. Moreover, since these s-PPs are produced with a living olefin polymerization, they are characterized by narrow molecular masses distribution and controlled values of the molecular weight, with a consequent expected effect on the elastic properties of s-PP.[39,40] The importance of studying the structure and mechanical properties of s-PP from these non-metallocene catalysts is related to the possibility to form with living olefin polymerization block copolymers having crystallizable polyolefin blocks, made of polyethylene or s-PP, with potential interesting properties. In this paper the structural characterization and analysis of the mechanical properties of this novel s-PP are reported, and the effect of different defects is discussed.

Experimental Section

The syndiotactic polypropylene sample sPP(PHI) was prepared as described in refs 20−22 using the bis(phenoxyimine)-titanium-based catalyst **2** of Chart 1 activated with MAO.

Microstructural analysis performed by solution ^{13}C NMR has revealed that the polymer sample is highly syndiotactic with fully syndiotactic pentad content [*rrrr*] = 90%. A chain-end control mechanism is operative, producing concentration of *m* dyads stereodefects of 3.6%. The microstructural characteristic and other physical properties of the sample are reported in Table 1. The polymer sample exhibits a melting temperature of 140 °C, a very high molecular weight M_n = 690 000 (M_w = 814 000), and a narrow molecular weight distribution (M_w/M_n = 1.18). As demonstrated in refs 21 and 22, these data and a lack of olefinic end groups in both the ^1H and ^{13}C NMR spectra indicate the living nature of the polymerization.

The structure and the physical properties of the sample sPP(PHI) have been compared with those of a s-PP sample

Table 1. Melting Temperatures, Molecular Masses (M_w), Polydispersity Indices (M_w/M_n), and Distribution of Pentads Stereosequences of Samples sPP(PHI), Prepared with Catalyst 2 of Chart 1, and Sample sPP(Cs), Prepared with the Classic C_s-Symmetric Metallocene Catalyst $(CH_3)_2C(Cp)(9\text{-Flu})ZrCl_2$/MAO

sample	T_m (°C)	M_w	M_w/M_n	[*mmmm*] (%)	[*mmmr*] (%)	[*rmmr*] (%)	[*mmrr*] (%)	[*rmrr*] + [*mmrm*] (%)	[*rmrm*] (%)	[*rrrr*] (%)	[*rrrm*] (%)	[*mrrm*] (%)
sPP(PHI)	140	814 000	1.18	0.5	0	0	0	3.6[a]	0.9	89.8	3.8	1.4
sPP(Cs)	146	164 000	2.2	0	0	1.7	2.7	1.6[a]	0	91.0	3.0	0

[a] In both samples the observed signals in the ^{13}C NMR spectra basically correspond to the pentad *rmrr*.

prepared with the C_s-symmetric metallocene catalyst isopropylidene(cyclopentadienyl)(9-fluorenyl)$ZrCl_2$ ($(CH_3)_2C(Cp)$-(9-Flu)$ZrCl_2$) activated with MAO,[31] having a similar stereoregularity (sample sPP(Cs)). The sPP(Cs) sample was polymerized at 80 °C, producing a highly syndiotactic polymer with a concentration of *rrrr* pentad of 91%, containing comparable amounts of *mm* triad and *m* dyad stereodefects and no measurable regiodefects. The microstructure and the physical properties of the sample sPP(Cs) are summarized in Table 1. This sample corresponds to sample s-PP(3) of ref 36.

The solution ^{13}C NMR spectrum of the s-PP samples were recorded on a Varian XL-200 operating at 50 MHz in the Fourier transform mode of 10% w/v polymer solutions in deuterated tetrachloroethane (also used as internal standard) at 125 °C.

Molecular weights (M_w and M_n) and polydispersity (M_w/M_n) were determined by high-temperature gel-permeation chromatography (GPC) in 1,2,4-trichlorobenzene at 140 °C relative to standard polystyrene.[21]

The calorimetric measurements were performed with a differential scanning calorimeter (DSC) Perkin-Elmer DSC-7 in a flowing N_2 atmosphere. The melting temperatures were taken as the peak temperature of the DSC curves.

The sample sPP(PHI) was isothermally crystallized from the melt at different temperatures. The as-prepared sample was melted at 200 °C and kept for 5 min at this temperature in a N_2 atmosphere; it was then rapidly cooled to the crystallization temperature, T_c, and kept at this temperature, still in a N_2 atmosphere, for a time t_c long enough to allow complete crystallization at T_c. The samples were then rapidly cooled to room temperature and analyzed by X-ray diffraction and differential scanning calorimetry. In the various isothermal crystallizations, the crystallization time t_c is different depending on the crystallization temperature. The shortest time is 24 h for the lowest crystallization temperature and increases with increasing the crystallization temperature, up to 2 weeks for the highest crystallization temperature.

The degree of order present in the structure of form I in the samples crystallized from the melt was evaluated from the measure of the ratio between the intensities of the 211 and 020 reflections, at $2\theta = 18.8°$ and 15.8°, respectively, $R = I(211)/I(020)$.[36] The intensities of 211 and 020 reflections were measured from the area of the corresponding diffraction peaks arising above the diffuse halo in the X-ray powder diffraction profiles.

Oriented fibers of the sample sPP(PHI) have been obtained by stretching at room temperature and at drawing rate of 10 mm/min compression-molded samples. Compression-molded films used for the measurements of the mechanical properties and the preparation of oriented fibers were obtained by melting the s-PP powder sample at 180 °C between perfectly flat brass plates under a press at very low pressure and slowly cooling to room temperature. Special care has been taken to obtain films with uniform thickness (0.3 mm) and minimize surface roughness, according to the recommendation of the standard ASTM D-2292-85.

X-ray diffraction patterns were obtained with Ni-filtered Cu Kα radiation. The powder profiles were obtained with an automatic Philips diffractometer, whereas the fiber diffraction patterns were recorded on a BAS-MS imaging plate (FUJIFILM) using a cylindrical camera and processed with a digital imaging reader (FUJIBAS 1800). The X-ray fiber diffraction patterns have been recorded for stretched fibers soon after the stretching and keeping the fiber under tension as well as for relaxed fibers, that is, after keeping the fiber under tension for 2 h and then removing the tension, allowing the complete relaxation of the specimens.

The index of crystallinity was evaluated from the X-ray powder diffraction profiles by the ratio of the crystalline diffraction area and the total area of the diffraction profile.

Solid-state ^{13}C NMR CPMAS spectra were recorded at room temperature on a Bruker AC-200 spectrometer, equipped with an HP amplifier ^1H 200 MHz, 120 W continuous wave, and with a pulse amplifier M3205. The samples (50 mg) were packed into 4 mm zirconia rotors and sealed with Kel-F caps. The spin rate was kept at 8.0 kHz, and the 90° pulse was 3.0 μs. The contact time for the cross-polarization, optimized in order to maximize the signals in the rigid (crystalline) regions of the samples, was 1 ms; the relaxation delay time was 4 s. Spectra were obtained with 1024 points in the time domain, zero-filled, and Fourier-transformed with size of 2048 points; 7200 scans were performed for each sample. Crystalline polyethylene was used as external reference at 33.6 ppm from tetramethylsilane.

Mechanical tests have been performed at room temperature on compression-molded films and oriented fibers of the sample sPP(PHI) with a miniature mechanical tester apparatus (Minimat, by Rheometrics Scientific), following the standard test method for tensile properties of thin plastic sheeting ASTM D882-83.

Mechanical tests have been first performed on the unstretched compression-molded films. Rectangular specimens 10 mm long, 5 mm wide, and 0.3 mm thick have been stretched up to the break or up to a given strain ϵ. Two benchmarks have been placed on the test specimens and used to measure elongation. Similar tests have been then performed at room temperature on the strained and then stress-relaxed fibers. Stress-relaxed fiber specimens have been prepared by stretching the compression-molded films of initial length L_0 up to strain of 500% (final length $L_f = 6L_0$), keeping the fibers under tension for 10 min at room temperature, and then removing the tension, allowing the specimens to relax.

Mechanical cycles of stretching and relaxation have been performed at room temperature on these stress-relaxed fibers, and the corresponding hystereses have been recorded. In these cycles the stress-relaxed fibers of the s-PP sample, having the new initial length L_r, have been stretched up to the final length $L_f = 6L_0$, i.e., up to the elongation $\epsilon = [(L_f - L_r)/L_r] \times 100$, and then relaxed at a controlled rate. The values of the tension set have been measured after each cycle according to the standard test method ASTM D412-87. The final length of the relaxed specimens L_r' has been measured 10 min after the end of the relaxation step, and the tension set has been calculated by using the following formula: $t_s(\epsilon) = [(L_r' - L_r)/L_r] \times 100$.

Values of tension set have been also measured on unoriented compression-molded films after breaking. Specimens of initial length L_0 have been stretched up to the break. Ten minutes after breaking the two pieces of the sample have been fit carefully together so that they are in contact over the full area of the break, and the final total length L_r of the specimen has been obtained by measuring the distance between the two benchmarks. The tension set at break has been calculated as $t_b = [(L_r - L_0)/L_0] \times 100$.

In the mechanical tests the ratio between the drawing rate and the initial length was fixed equal to 0.1 mm/(mm × min) for the measurement of Young's modulus and 10 mm/(mm × min) for the measurement of stress−strain curves and the determination of the other mechanical properties (stress and strain at break and tension set). The reported values of the

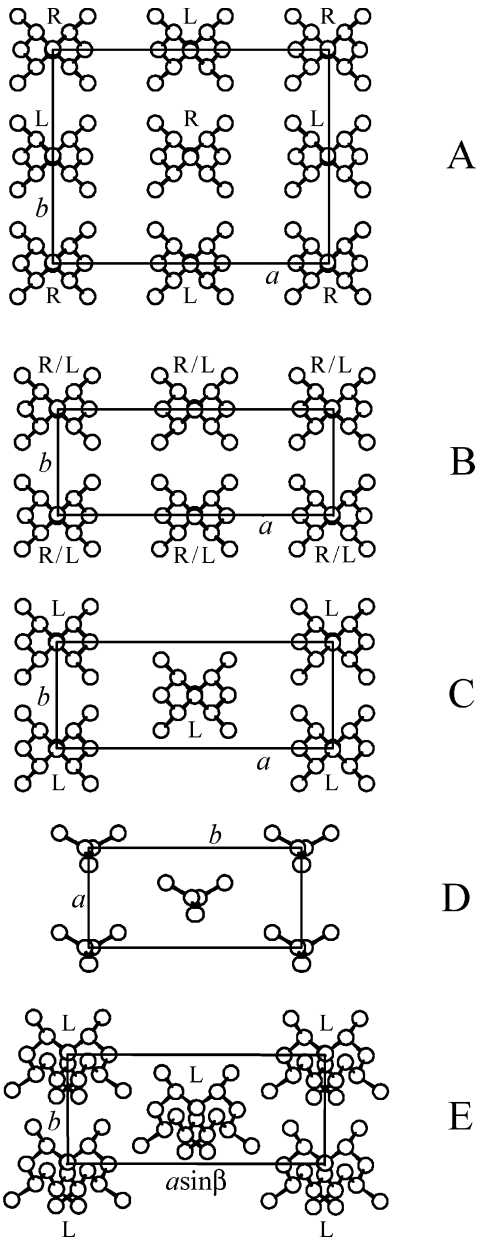

Figure 1. Models of packing of the limit ordered form I (A), the limit disordered form I (B), form II (C), form III (D), and form IV (E) of s-PP. R = right-handed helix; L = left-handed helix.

mechanical properties are averaged over at least five independent experiments.

Results and Discussion

Structural Characterization. Powder Samples. The structure and properties of syndiotactic polypropylene produced with single center metallocene catalysts have been extensively studied.[36−48] In particular, deep analyses of the crystallization behavior and mechanical properties have been reported either for s-PP prepared with C_s-symmetric catalysts, based on zirconium complexes bearing cyclopentadienyl and fluorenyl ligands,[31] having medium-high stereoregularity ([*rrrr*] > 80%),[36−48] or for high molecular weight s-PP having low syndiotacticity ([*rrrr*] = 50−60%),[49−51] prepared with constrained geometry catalysts.[52]

A very complex polymorphic behavior has been described. Four different crystalline forms,[36−48] shown in Figure 1, and a mesomorphic form[53−55] have been found. The most stable form I (Figure 1A,B) and the metastable form II (Figure 1C) are characterized by chains in **s**(2/1)2 helical conformation, packed in orthorhombic unit cells.[36,37,41,44,56] The two metastable modifications, form III (Figure 1D) and form IV (Figure 1D), present chains in trans-planar[42] and $(T_6G_2T_2G_2)_n$[43,47] helical conformations, respectively.

A polymorphic transition between the trans-planar form III and the isochiral helical form II has been observed in oriented fibers.[37,39,40,48] The trans-planar form III can be obtained by stretching at room temperature highly stereoregular s-PP samples[42,44] and transforms into the isochiral helical form II upon releasing the tension.[37,39,40,48] This transition is reversible; the trans-planar form III and the helical form II transform each other by stretching and relaxing oriented fibers.[40]

The formation of the four crystalline modifications depends on the condition of crystallization and the stereoregularity of the sample.[36−40,44,55] As-prepared and melt-crystallized samples of s-PP having high degree of stereoregularity (with [*rrrr*] higher than 90%) always crystallize in the most stable form I (Figure 1A,B).[36,41,44,46] As shown in ref 36, form I of s-PP crystallizes from the melt in different modifications characterized by variable amounts of disorder depending on the crystallization temperatures. The limit ordered modification of form I, characterized by a regular alternation of right- and left-handed 2-fold helical chains along both axes of the unit cell (Figure 1A),[41] is obtained at high values of the crystallization temperature. For lower stereoregular samples, with [*rrrr*] in the range 88−75%, disordered modifications of form I, characterized by disorder in the alternation of right- and left-handed helical chains along the axes of the units cell (Figure 1B), are always obtained by melt-crystallization, even at high crystallization temperatures.[37,38]

Different polymorphic behaviors in samples having different stereoregularities have been observed also in oriented fibers.[37,39] The pure trans-planar form III (Figure 1D) is, indeed, obtained only for highly syndiotactic samples ([*rrrr*] higher than 90%) by stretching compression-molded films at room temperature[37,39,42,44] or by cold-drawing at temperatures below the glass transition temperature.[42,44,57] The lower the syndiotacticity, the more difficult is the formation of the trans-planar form III by stretching.[37,38] In the case of very low stereoregular s-PP samples prepared with constrained geometry catalysts, with *rrrr* contents in the range 40−50%, the trans-planar form III is never observed in stretched fibers, and only the disordered mesomorphic form can be obtained by stretching.[49−51] The different polymorphic behavior upon stretching is most probably linked to the different amounts of defects of stereo- and regioregularity of the chains. It has been suggested that defects of stereoregularity and, probably, even regioregularity are highly tolerated within the lattices of the crystalline modifications of s-PP with chains in helical conformation,[37,39,45] whereas such defects would be hardly included in the crystalline lattice of the trans-planar form III. Great influence of the *mm* triad or *m* dyad stereodefects on the crystallization of the isochiral helical form II, in both powder and fiber samples, has been also suggested.[37]

These data indicate that different types of defects of stereoregularity and/or regioregularity may give different influences on the polymorphic behavior and, as a consequence, on the physical properties of s-PP.

Table 2. Chemical Shifts of Resonances Observed in the ^{13}C NMR Spectrum of the Sample sPP(PHI) of Figure 2, Corresponding to Carbon Atoms in the Regioirregular Sequences of Chart 2[a]

carbon	designation	chemical shift (ppm)	carbon	designation	chemical shift (ppm)
1′	$P_{\alpha,\beta(threo)}$	14.6−15.8	7	$T_{\beta,\gamma}$	31.1
1	$P_{\alpha,\beta(erythro)}$	16.6−17.4	9	$S_{\gamma\alpha,\alpha\delta}$	41.5−42.4
2	$T_{\alpha,\beta}$	34.2−36.5	13	$T_{\alpha,\gamma}$	38.4−39.0
2′	$T_{\alpha,\beta}$	34.2−36.5	14	$S_{\beta\alpha,\beta\delta}$	32.5
3	$S_{\gamma\alpha,\alpha\beta}$	43.0−44.6	15	$S_{\gamma\alpha,\beta\gamma}$	34.2−36.5
6	$S_{\gamma\alpha,\beta\delta}$	34.2−36.5	16	$S_{\beta\alpha,\alpha\gamma}$	41.5−42.4

[a] The designation of methyl, methylene, and methine carbon atoms is also reported.[58]

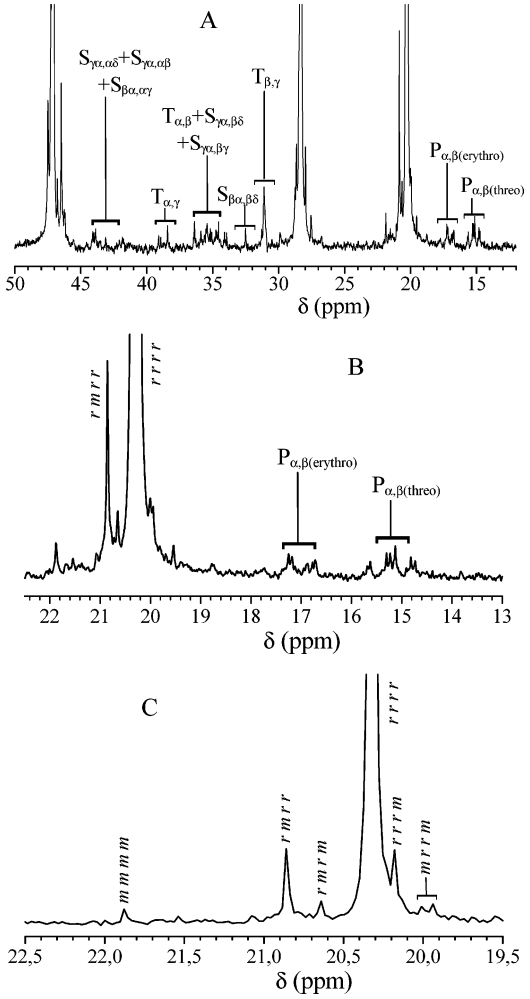

Figure 2. Solution ^{13}C NMR spectrum of the sample sPP-(PHI) prepared with the catalyst **2** of Chart 1 (A). Regions of the spectrum of the methyl carbon atoms resonance (B,C). The resonances of methyl (B) and methylene carbon atoms (A) in regiodefective sequences (Chart 2 and Table 2) and the assignment of methyl signals to pentads stereosequences (C) are also shown.

The solution ^{13}C NMR spectrum of the sample sPP-(PHI), prepared with the bis(phenoxyimine)titanium-based catalyst **2** of Chart 1, is reported in Figure 2. The main resonances observed in the region of methyl carbon atoms are at 20.85, 20.32, and 20.19 ppm, which correspond to the *rrmr*, *rrrr,* and *rrrm* pentad stereosequences. The concentrations of pentads are reported in Table 1. The ratio of concentrations of pentads *rrrm* and *rrmr* is nearly 1, consistent with the chain-end mechanism of stereocontrol,[20−22] with a content of *m* dyads defects of 3.6% (Table 1).

Moreover, the spectrum of Figure 2 also presents less intense and broad resonances in the ranges 14.6−15.8 and 16.6−17.4 ppm, corresponding to vicinal threo and erythro methyl carbon atoms,[58] respectively, in the range 34−36.4 ppm, corresponding to vicinal methylene carbon atoms and vicinal threo and erythro methine carbon atoms,[58] and in the range 41.5−44.6 ppm, corresponding to methylene carbon atoms close to vicinal methine or methylene groups. This indicates the presence of defects of regioregularity, due to primary (1,2) insertions in a prevailingly secondary (2,1) enchainment.[21,22] These resonances are spread between 14−17, 34−36, and 41−45 ppm because of the stereoirregular environment. The assignment of the resonances present in the spectrum of Figure 2, arising from the regioirregular sequences shown in Chart 2, is reported in Table 2 according to the designation of ref 58. From the intensities of the $P_{\alpha,\beta}$ signals an amount of nearly 2% of defects of regioregularity has been evaluated.

Chart 2. Fischer Projections of Regioirregular Sequences in Polypropylene Chains

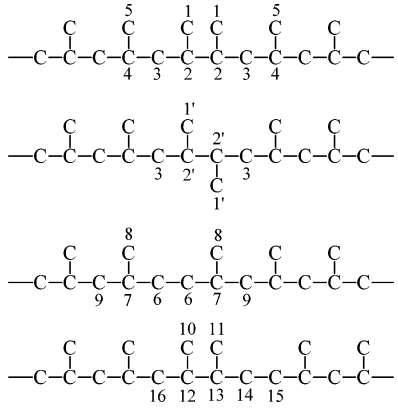

The X-ray powder diffraction profile and the solid-state ^{13}C NMR CPMAS spectrum of the as-prepared sample sPP(PHI) are shown in Figure 3. The diffraction profile (Figure 3A) presents both 020 and 110 reflections at $2\theta = 16°$ and 17°, respectively, typical of the antichiral helical form I (Figure 1A) and isochiral form II (Figure 1C), respectively.[41,44,46,56] This indicates that the as-prepared sample is crystallized in mixture of the two polymorphic helical forms. It is worth noting that the isochiral helical form II is generally obtained only in stretched fibers of s-PP,[37,56] whereas powder samples crystallized from the melt or solutions are always in the antichiral form I.[44] Only in special conditions, that is for low stereoregular s-PP samples, quench precipitated from solutions, conformationally disordered modifications of form II have been crystallized in powder samples.[59] The result of Figure 3 indicates that the sample sPP(PHI) obtained with the phenoxyimine catalyst provides a rare example of crystallization of the isochiral helical form II in powder samples of s-PP.

The solid-state CPMAS ^{13}C NMR spectrum of the as-prepared sample sPP(PHI) (Figure 3B) is characterized

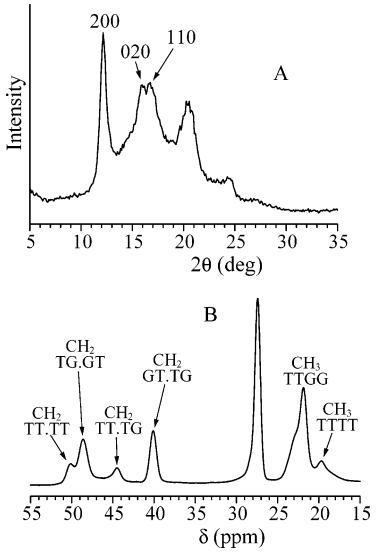

Figure 3. X-ray powder diffraction profile (A) and solid-state ^{13}C NMR CPMAS spectrum (B) of the as-prepared sample sPP(PHI) prepared with the catalyst **2** of Chart 1.

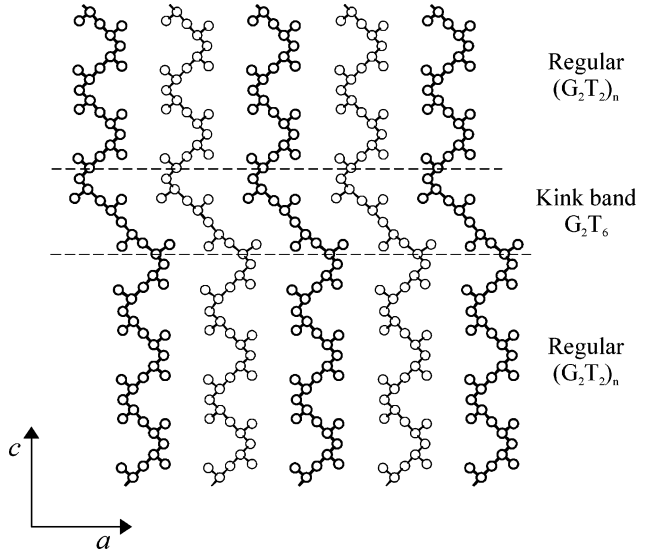

Figure 4. Model for the conformationally disordered modifications of form II of s-PP containing kink bands. The chains are in a prevailing 2-fold helical conformation with defects characterized by trans-planar conformational sequences. The defective portions of the chains are clustered in planes, delimitated by the dashed lines, and correspond to conformational sequences G_2T_6. The chains are packed like in the form II of s-PP, the helical portions of the chains being isochiral. The chains drawn with thick and thin lines are at $b = 0$ and 0.5, respectively.

by the usual resonances of methyl, at $\delta = 21.9$ ppm, methine, at 27.4 ppm, and methylene carbon atoms, at 40.0 and 48.6 ppm, typical of the 2-fold $(TTGG)_n$ helical conformation of s-PP,[60] and by additional resonances at $\delta = 19.7$ and 22.7 ppm, for the methyl carbon atoms, and at $\delta = 44.5$ and 50.1 ppm for the methylene carbon atoms.

These features are similar to those present in the spectra of low stereoregular s-PP samples quench-precipitated from solutions and crystallized in kink-bands disordered modifications of form II, described in recent papers.[59] We have indeed interpreted the presence of these additional resonances with the presence of conformational disorder of the chains in the crystalline phase, which originates from the presence of trans-planar sequences in chains having a prevailing 2-fold $(TTGG)_n$ helical conformation.[59] In particular, the resonance at $\delta = 44.5$ ppm was assigned to CH_2 groups in a TT.TG or GT.TT conformational environment, which experience one γ-gauche effect (the dots indicate the methylene carbon atoms), whereas the resonance at 19.7 and 50.1 ppm was assigned to methyl and methylene carbon atoms, respectively, in portions of chains in trans-planar TTTT conformation,[59] according to the resonances found for the trans-planar form III of s-PP.[61] Finally, the resonance at 22.7 ppm could be attributed to methyl carbon atoms placed at the interface between the trans-planar and the helical portions of chains or belonging to the noncrystalline phase.[59]

The presence of these additional resonances in the spectrum of Figure 3B indicates that crystals of form II obtained in mixture with form I in the as-prepared sample sPP(PHI), as evidenced by the diffraction profile of Figure 3A, are actually in the kink-bands conformationally disordered modifications of form II, like, for instance, that shown in the model of Figure 4.[59] In this model portions of chains in ordered **s**(2/1)2 helical conformation, having the same chirality, are connected by portions of chains in trans-planar conformation (in the most probable model this portions of chain are T_6 sequences), producing kink-bands defects in G_2T_6 conformation. According to this model, each chain containing a kink-band G_2T_6 defect contains two methylene groups in a GT.TT conformational environment, giving the resonance at 44.5 ppm, one methylene group in a TT.TT sequence, one methylene carbon atom in a TG.GT sequence, and two methyl groups in TTTT sequences, corresponding to the resonances at ≈50, ≈49, and 19.7 ppm, respectively. The ratio between the intensity of the methylene resonance at 44.5 ppm and that of the resonance of the methyl groups in TTTT sequences at 19.7 ppm should be nearly 1, according with the intensities observed in the experimental spectrum of Figure 3B.

It is worth noting that kink-bands disordered modifications of form II of the kind of Figure 4 have also been observed in as-prepared samples of syndiotactic propylene−ethylene copolymers.[62] The formation of these disordered modifications is easier in the copolymers than in the case of the s-PP homopolymer prepared with the same C_s-symmetric catalysts because it is kinetically favored by the easier local formation of trans-planar sequences in the presence of ethylene units.[62] The inclusion of ethylene comonomeric units in the crystalline regions of copolymers favors, locally, the formation of trans-planar sequences, which, in turn, induces the crystallization of the samples in disordered modifications of form II containing kink-bands.[62]

The data of Figure 3 clearly indicate that the sample sPP(PHI) produced with the phenoxyimine-based catalyst **2** of Chart 1 presents a crystallization behavior similar to that of the propylene−ethylene copolymers, since kink-bands disordered modifications of form II are more easily obtained in the as-prepared sample than in the case of s-PP prepared with C_s-symmetric metallocene catalysts. This is probably due to the presence of nonnegligible amount (about 2%) of defects in the regular secondary (2,1) enchainment, which produce vicinal methylene carbon atoms $-CH_2-CH_2-$, due to secondary (2,1) insertion into a primary metal−alkyl bond (after a primary (1,2) insertion).[21,22] The presence of pairs of methylene groups along the polymer chains

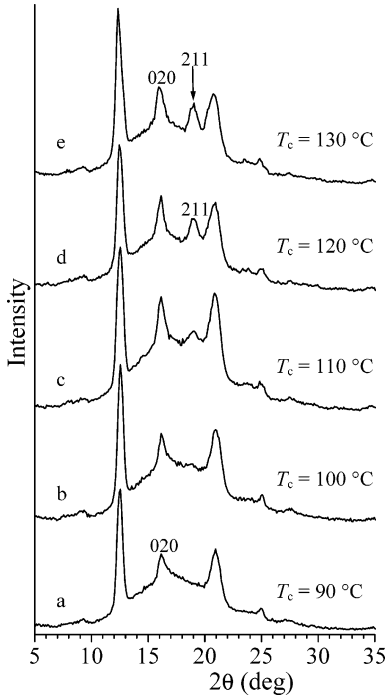

Figure 5. X-ray powder diffraction profiles of specimens of the sample sPP(PHI) isothermally crystallized from the melt at the indicated crystallization temperatures T_c. The 020 and 211 reflections at $2\theta = 16°$ and 18.8°, respectively, of form I are also indicated.

probably favors, locally, the formation of trans-planar sequences, which, in turn, induces the crystallization of the sample in the kink-bands disordered modification of form II of Figure 4.

The X-ray powder diffraction profiles of samples obtained by isothermal crystallizations from the melt at various temperatures T_c of the sample sPP(PHI) are reported in Figure 5. It is apparent that, while the as-prepared sample is crystallized in the kink-bands disordered modification of form II (Figures 3 and 4), the sample crystallizes from the melt at any temperature in the stable antichiral form I (Figure 1A,B). This is demonstrated by the presence of the 200, 020, and 211 reflections at $2\theta = 12.2°$, 16°, and 18.8°, respectively, typical of the antichiral form I (Figure 1A),[36,41] and the absence of the 110 reflection at $2\theta = 17°$, typical of the isochiral helical form II (Figure 1C),[44,56] in the diffraction profiles of Figure 5. As observed for the metallocene s-PPs,[59] and for propylene−ethylene copolymers,[62] the kink-bands disordered modifications of form II (Figure 4) are metastable and can be obtained only in the as-prepared samples by fast crystallization from the reaction medium. After melting and successive crystallization the stable antichiral form I is obtained (Figure 5).

The data of Figure 5 indicate that at low crystallization temperatures disordered modifications of form I, characterized by a statistical disorder in the positioning of right- and left-handed helical chains (Figure 1B), are formed, as demonstrated by the absence and/or the low intensity of the 211 reflection at $2\theta = 18.8°$ in the X-ray powder diffraction profiles of Figure 5a,b. We recall that the 211 reflection at $2\theta = 18.8°$ is typical of the packing characterized by the regular alternation of 2-fold helices of opposite chirality along the *a* and *b* axes (Figure 1A).[36,41,46] This reflection is present only in the X-ray diffraction profiles of the samples crystallized at high temperatures, and its intensity increases with increasing the crystallization temperature (Figure 5c−e). The diffraction profiles of Figure 5 indicate that with increasing the crystallization temperature crystals of form I of s-PP, characterized by a certain degree of order in the alternation of right- and left-handed helices along the axes of the unit cell, are obtained. Quite ordered modifications of form I of s-PP are formed only at high crystallization temperatures. However, even at the highest crystallization temperature, the intensity of the 211 reflection is still lower than that expected for the limit ordered structure of form I of s-PP.[36] This indicates that for the sample sPP(PHI) the ordering process in the alternation of right- and left-handed helices along the axes of the unit cell and the formation of the ideally ordered antichiral form I of Figure 1A[36,41] are prevented.

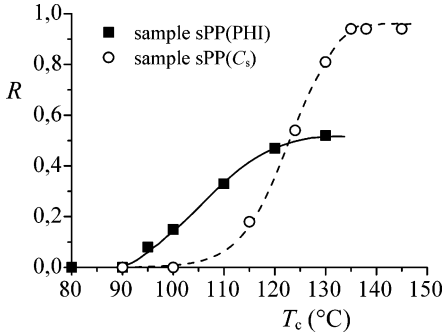

Figure 6. Values of the order parameter R of s-PP samples crystallized from the melt are reported as a function of the crystallization temperature T_c: (■) sample sPP(PHI) from nonmetallocene octahedral catalyst **2** of Chart 1; (○) sample sPP(Cs) from C_s-symmetric metallocene catalyst (data from ref 36).

The intensity of the 211 reflection at $2\theta = 18.8°$ can be used as a measure of the degree of order present in the crystals of form I.[36] Precisely, since the intensity of the 020 reflection is constant with T_c, we use the ratio between the intensities of 211 and 020 reflections, at $2\theta = 18.8°$ and 16°, respectively, $R = I(211)/I(020)$, to eliminate any dependence of the diffraction intensity on the crystallinity and the thickness of the samples.[36] The values of R of the melt-crystallized samples are reported in Figure 6 as a function of the crystallization temperature and compared with the values of R of the sample sPP(Cs), prepared with the common C_s-symmetric metallocene catalyst, having similar stereoregularity ([*rrrr*] = 91%), taken from the ref 36.

It is apparent that, while for the metallocene-made s-PP the order parameter R increases with T_c from $R = 0$, corresponding to the limit disordered structure of form I, characterized by a statistical positioning of right- and left-handed helical chains in each site of the lattice (Figure 1B), to a constant value $R \approx 1$, corresponding to the limit ordered structure of form I (Figure 1A),[36] for the nonmetallocene sample sPP(PHI) the limit values of R is lower than 1 and approaches to about 0.5.

In recent papers we have demonstrated that the maximum degree of structural order in the alternation of right- and left-handed helical chains in the stable form I that can be achieved by melt-crystallizations depends on the stereoregularity of the sample.[36,37,51] Form I of s-PP, indeed, crystallizes from the melt in different modifications characterized by variable amounts of disorder depending on the crystallization temperature and stereoregularity. For low stereoregular s-PP samples, with [*rrrr*] lower than 80%, disordered modifications of form I, characterized by disorder in the alternation of

right- and left-handed helical chains along the axes of the units cell (Figure 1B), are always obtained by melt-crystallization, even at high crystallization temperatures.[37,38,51] In these samples, small amounts of crystals of form II are present[37] and/or a mode of packing of form II occurs as a defect in a prevailing mode of packing of form I.[37,38] This kind of defect corresponds to a disorder in the stacking of *bc* layers of chains along the *a* axis, implying *b*/4 shifts among consecutive *bc* layers piled along *a*.[41,45] Less stereoregular samples are therefore not able to crystallize from the melt in the ordered form I, owing to the tendency to form local arrangements of the chains as in form II.[37,38]

The data of Figures 5 and 6 indicate that, even though the sample sPP(PHI) from phenoxyimine-based catalyst and the metallocene-made sample sPP(Cs) present similar relatively high stereoregularity ([*rrrr*] = 90−91%), their polymorphic behavior is completely different. In the sample sPP(PHI) the formation of the ordered antichiral packing is prevented even at high crystallization temperatures. This different behavior is probably related to the different microstructures of the two samples, that is, the different types of microstructural defects produced by the different catalysts. As discussed above, the sample sPP(PHI) prepared with the catalyst of Chart 1 is mainly characterized by the presence of significant amount (3.6%) of isolated *m* dyads stereodefects, due to the chain-end stereocontrol, and of about 2% of regiodefects, due to primary insertion of the monomer in a prevailingly secondary (2,1) enchainment. The metallocene-made sample sPP(Cs) is instead characterized by lower amount (1.7%, Table 1) of isolated *mm* triads and *m* dyads stereodefects, and no measurable regiodefects are generally observed.[31]

The effects of the presence of stereodefects on the ordering of the position of right- and left-handed helical chains in the form I of s-PP may be explained considering the modeling of the origin of disorder in the various polymorphic forms of s-PP proposed by us some years ago.[45] We argued that the experimental evidence that s-PP may crystallize in statistically disordered modifications of both helical forms I and II, as for instance the structure of Figure 1B for form I (described by the statistical space group *Bmcm*),[36] implying that chains of opposite chirality may be found with the same probability in each site of the lattice, poses the question of whether each single macromolecular chain may take successively right- and left-handed helical conformations along the chain axis, while maintaining a correlation in the position of the methyl groups. We have suggested that such inversions of the chirality of the helical conformation may occur along a single macromolecular chain in correspondence of *m* dyads defects of stereoregularity (i.e., for ...*rrrmrrr*... sequences). A model of conformational inversion in a s-PP chain pinned to a *m* dyad defect is shown in Figure 7A.[45]

In this model it is assumed that right- and left-handed portions of the chain are connected by the *m* defect and are coaxial. Low conformational energy is achieved by slight distortions of the torsion angles of bonds around the *m* defects from the gauche value. The sequence of torsion angles in the model of Figure 7A is, indeed, ...$(G^-G^-TT)_n(G'G'')(TTG^+G^+)_m$..., where G′ and G″ are torsion angles slightly deviated from the G^- value. The positions of the methyl groups belonging to the two enantiomorphic portions of chain, a few atoms beyond the defect, are at the proper crystallographic positions

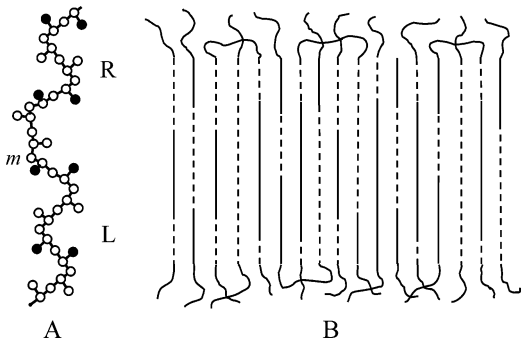

Figure 7. (A) Model of inversion of the chirality in the **s**(2/1)2 helical conformation of s-PP. The conformational inversion corresponds to an inversion in the succession of configurations and occurs in correspondence of configurational defect of the kind *rrrrmrrrr*. Left (L)- and right (R)-handed helical portions of the s-PP chain are connected by the *m* dyad defect and are coaxial, while the methyl groups on both sides of the conformational inversion are in register with the crystallographic positions. (B) Schematic model of a crystal of s-PP with long chains containing inversions in the helical chirality. Helices of opposite chirality (right and left) are indicated with solid and dashed lines. In the crystal there may be a core of helices packed with opposite chirality in the short range, as in the form I. The correlation between the chirality is lost at long distances.

so that methyl carbon atoms are well interdigitated with those of adjacent chains, at a low cost of free energy.[45] Such type of defects are, therefore, probably tolerated within the crystals of s-PP. In such crystals, however, even in the case that one or more inversions of helical chirality are present along each chain axis, we can always imagine a core of the crystal where a strong correlation between chiralities of neighboring chains is maintained in the short range, and more external parts, in which the precise correlation fades away and, finally, disappear at long distances. A possible model of the crystal is shown in Figure 7B. The crystals are constituted by blocks characterized by a core where some kind of short-range order in the alternation of right- and left-handed helical chains (corresponding to a limit ordered structure of form I of Figure 1A) is achieved. At the periphery of the blocks the higher level of order of the core may fade out (because configurational errors along the chain cause inversions in the sense of spiralization), while only the order in the parallelism of the chains, corresponding to a limit disordered structure of Figure 1B, is maintained. The lower degree of order may be maintained at longer distances within each block and among different blocks within each single crystal.

The presence of *m* defects in the sample sPP(PHI) may induce inversions of the helical chirality along the chains, as in the model of Figure 7. Since the macromolecular chains are very long, due to the very high molecular weight produced by the living polymerization, the occurrence of a not negligible amount of inversions is expected. As a consequence, correlations at long distances between the chirality of the helices along *a* and *b* axes of the unit cell are destroyed. This produces departure from the fully antichiral packing of form I of Figure 1A, introducing disorder in the regular alternation of right- and left-handed helical chains. Antichiral packing of first neighboring chains may still be preserved locally and lost in the long range, preventing the formation of the fully ordered form I of Figure 1A.

The presence of defects of regioregularity may also play a role. As also found for syndiotactic propylene−

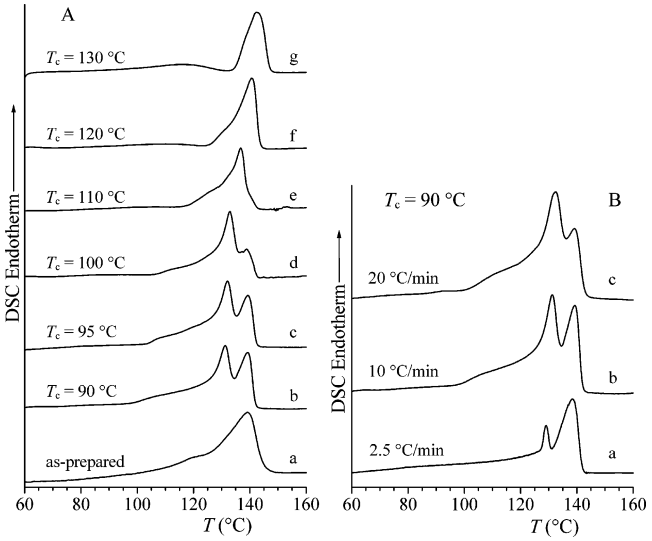

Figure 8. DSC heating curves, recorded at heating rate of 10 °C/min of specimens of the sample sPP(PHI) isothermally crystallized from the melt at the indicated crystallization temperatures T_c (A). DSC heating curves of the sample sPP(PHI) isothermally crystallized from the melt at T_c = 90 °C recorded at the indicated heating rates (B).

ethylene copolymers,[62] the presence of vicinal methylene groups (ethylene units in the copolymers), produced by (1,2) misinsertions, may induce the development of disorder in the stacking of *bc* layers of chains piled along *a*, characterized by shift of *bc* layers of *b*/4 along *b* (*b*/4 shifts disorder),[36,41] which in turn produces local arrangement of the chains as in the *C*-centered form II of s-PP (Figure 1C). Also, this kind of disorder, already observed for metallocene-made s-PP samples crystallized at low temperature,[41,36] destroys any correlation at long distances between the chirality of the helices along the *a* and *b* axes of the unit cell, preventing the crystallization of the fully ordered antichiral form I of Figure 1A.

The DSC melting curves of samples crystallized from the melt of Figure 5 are reported in Figure 8A in comparison with the DSC curve of the as-prepared sample sPP(PHI). It is apparent that the as-prepared powder presents a melting temperature (about 140 °C, curve a of Figure 8A) higher than those of the samples crystallized from the melt (curves b−f of Figure 8A). Only at the highest crystallization temperature of 130 °C a slightly higher melting temperature of 143 °C (curve g of Figure 8A) is obtained. Moreover, for the melt-crystallized samples only a slight increase of the melting temperature with increasing crystallization temperature is observed. Therefore, crystals of form I of the sample sPP(PHI) obtained by melt-crystallization present low melting temperatures, even at high crystallization temperatures, lower than those of crystals of form I of metallocene-made s-PP samples with similar stereoregularity.[38] This is in agreement with the model of Figure 7 and the X-ray diffraction results of Figures 5 and 6 that disordered crystals of form I of the sample sPP(PHI) always crystallize from the melt and no improvement of the degree of order is achieved with increasing crystallization temperature. The presence of helix reversals probably also prevents a great increase of lamellar thickness with increasing crystallization temperature.

It is worth noting that the DSC curves of samples crystallized at low crystallization temperatures (90−100 °C) present melting endotherms with multiple peaks (curves b−d of Figure 8A). This is due to the occurrence of recrystallization phenomena during heating, as demonstrated by the DSC scans of the sample crystallized at 90 °C recorded at different heating rates, shown as an example in Figure 8B. It is apparent that the area of the peak at high temperature decreases, whereas that of the peak at low temperature increases, with increasing heating rate, as expected for the presence of recrystallization during melting. At high heating rates less amount of melted material is, indeed, able to recrystallize during heating and the area of the high-temperature peak, corresponding to the melting of the recrystallized material, decreases (Figure 8B).

Oriented Fibers. Fibers of the sample sPP(PHI) have been prepared by stretching at room temperature and at drawing rate of 10 mm/min compression-molded samples. The X-ray fiber diffraction patterns of fiber specimens of the sample sPP(PHI), obtained by stretching at different values of deformation, and keeping the fiber under tension, are reported in Figure 9. The corresponding intensity profiles read along the equatorial line are also reported in Figure 9. It is apparent that the helical form I present in the initial unstretched melt-crystallized compression-molded sample (Figure 5) rapidly transforms into the trans-planar form III by stretching already at low values of deformation. The intensity of the 200 reflection at $2\theta = 12°$, typical of the helical form I (see Figure 5), indeed, has become very low already at 100% deformation (Figure 9A′) and further decreases with increasing deformation and finally disappears at high values of the strains (Figure 9D). Correspondingly, the equatorial $(020)_t$, $(110)_t$, and $(130)_t$ reflections at $2\theta = 16°$, 18°, and 30°, respectively, of the trans-planar form III, along with reflections on the first layer line corresponding to the trans-planar conformation periodicity (c = 5.1 Å), appears already at 100% deformation (Figure 9). The intensities of these reflections increase with increasing deformation, and fibers in the pure trans-planar form III are obtained at 500% deformation (Figure 9D).

These data indicate that in this sample the trans-planar form III can be obtained more easily than in the case of metallocene-made s-PP samples with similar stereoregularity.[39,40,48]

The X-ray fiber diffraction patterns and the corresponding diffraction profiles read along the equatorial line of fibers stretched at 100 and 500% deformations, kept in tension and after releasing the tension, are reported in Figures 10 and 11, respectively. In the case of the fiber stretched at 100% strain, which is basically in the trans-planar form III with small amount of the helical form I (Figure 10A), a partial loss of the orientation of crystals of the helical form is observed after releasing the tension (Figure 10B). Moreover, an increase of the intensity of the 200 reflection at $2\theta = 12°$ of the helical form is observed after removing the tension (Figure 10B′). These data indicate that crystals of trans-planar form III transform into helical form upon releasing the tension. The presence in the equatorial diffraction profile of Figure 10B′ of a broad reflection centered at $2\theta = 17°$ and the absence of any diffraction peak at $2\theta = 16°$ indicates that the helical form obtained is the isochiral helical form II (Figure 1C). However, the diffraction pattern of Figure 10B still presents a weak reflection on the first layer line corresponding to

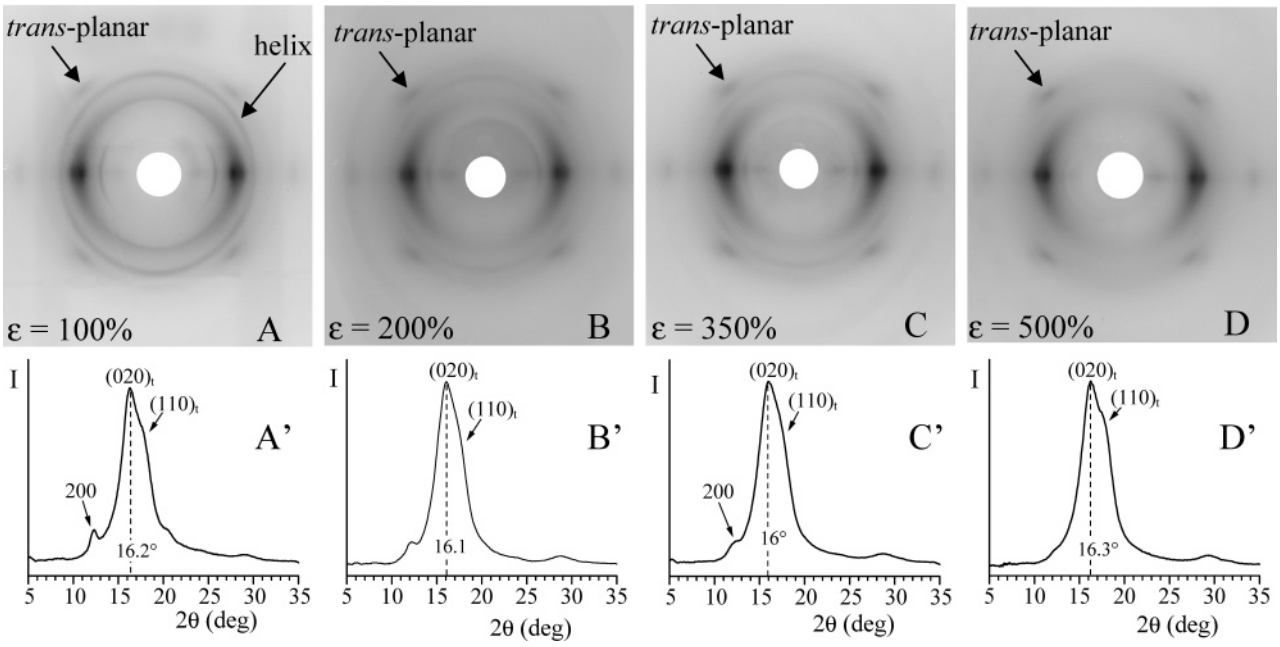

Figure 9. X-ray fiber diffraction patterns (A−D), and corresponding diffraction profiles read along the equator (A′−D′), of fibers obtained by stretching compression-molded films of the sample sPP(PHI) at room temperature up to different deformations ϵ. The 200 reflection of the helical form I, the $(020)_t$ and $(110)_t$ reflections of the trans-planar form III are indicated. On the first layer line reflections arising from the diffraction of crystals of helical and trans-planar mesomorphic forms and of form III ($(021)_t$, $(111)_t$ reflections) are also indicated.

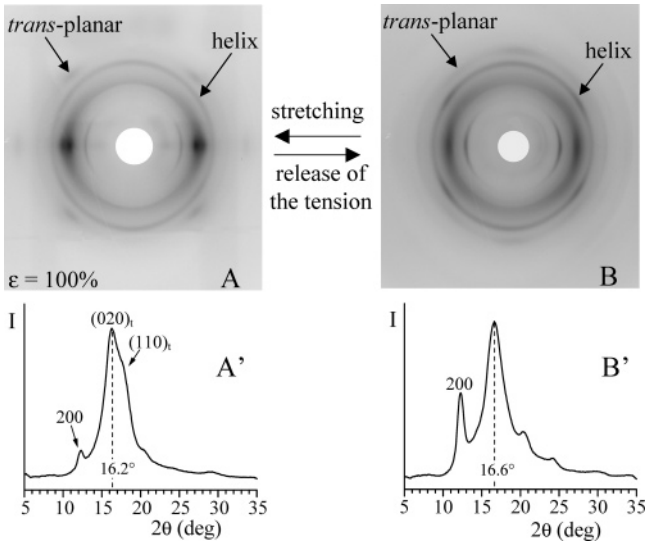

Figure 10. X-ray fiber diffraction patterns (A, B) and corresponding profiles read along the equatorial lines (A′, B′), of fibers of the sample sPP(PHI) obtained by stretching compression-molded films at 100% elongation, keeping the fiber under tension (A) and after removing the tension (B). The 200 reflection at $2\theta = 12°$ typical of the helical form, and the $(020)_t$ and $(110)_t$ reflections at $2\theta = 16°$ and 18°, respectively, of the trans-planar form III, are indicated.

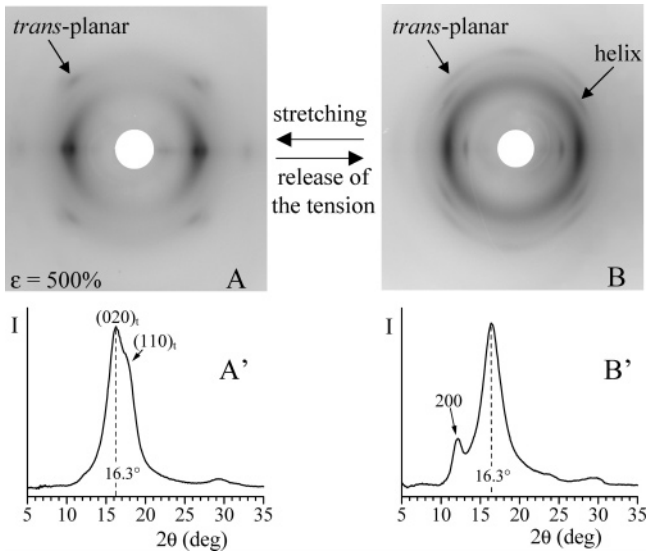

Figure 11. X-ray fiber diffraction patterns (A, B) and corresponding profiles read along the equatorial lines (A′, B′), of fibers of the sample sPP(PHI) obtained by stretching compression-molded films at 500% elongation, keeping the fiber under tension (A) and after removing the tension (B). The 200 reflection at $2\theta = 12°$ typical of the helical form, and the $(020)_t$ and $(110)_t$ reflections at $2\theta = 16°$ and 18°, respectively, of the trans-planar form III, are indicated.

the trans-planar conformation. This indicates that a fraction of crystals remains in the trans-planar form after removing the tension. The presence of the broad equatorial reflection at $2\theta = 17°$ in the pattern of Figure 10B indicates that these trans-planar crystals are in the mesomorphic form.[53−55] Therefore, the removal of the tension from 100% deformation produces transformation of a fraction of crystals of the trans-planar form III into the helical form II, while a fraction of crystals of form III remains in the trans-planar conformation but transforms into the disordered mesomorphic form.

As discussed above, for higher values of deformation fibers in the pure trans-planar form III are obtained (Figure 9D). The diffraction pattern of the fiber stretched at 500% deformation after releasing the tension (Figure 11B) presents on the equator a very weak 200 reflection at $2\theta = 12°$ of the helical form and a broad diffraction peak at $2\theta = 16.3°$, along with reflections on the first layer line corresponding to both helical and trans-planar conformations. Also in this case the trans-planar form III (Figure 11A) transforms into the helical form and into the trans-planar mesomorphic form (Figure 11B).

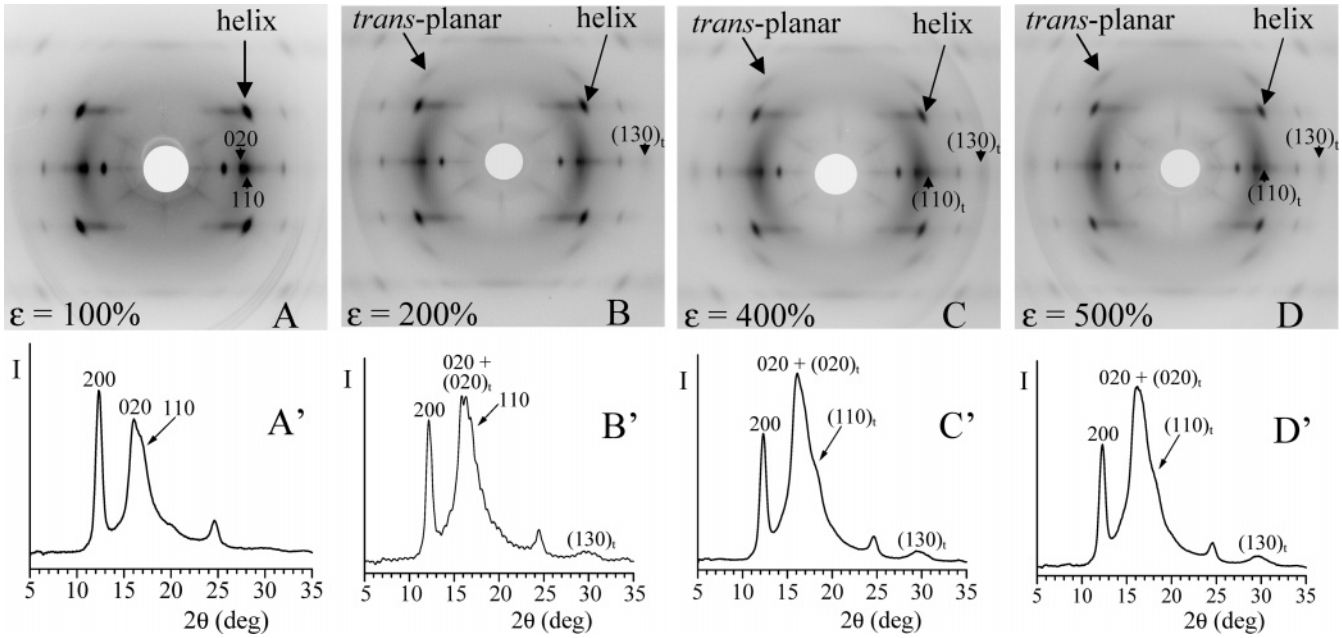

Figure 12. X-ray fiber diffraction patterns (A−D) and corresponding diffraction profiles read along the equator (A′−D′), of fibers obtained by stretching the sample sPP(PHI) at room temperature up to different deformations ϵ and annealed at 110 °C for 20 min. The 200 reflection at $2\theta = 12.2°$ of the helical forms, the 020 reflection at $2\theta = 16°$, and the 110 reflection at $2\theta = 17°$ of helical forms I and II, respectively, the $(020)_t$, $(110)_t$, and $(130)_t$ reflections at $2\theta = 16°$, 18°, and 30° of the trans-planar form III are indicated. On the first layer line reflections arising from the diffraction of crystals of helical forms and trans-planar form III are also indicated.

The intensity of the 200 reflection at $2\theta = 12°$ of the helical form is lower than that observed in the diffraction pattern of the fiber relaxed from 100% deformation of Figure 10B′. The amount of helical form obtained from the trans-planar form III by releasing the tension is lower when the fibers are stretched at higher deformation. In this condition crystals of form III formed by stretching transform only marginally into the helical form; they mainly remain in the trans-planar conformation and only transform into the disordered mesomorphic form. These data indicate that in the sample sPP(PHI) the stretching at high deformations stabilizes the trans-planar forms (form III and/or mesomorphic from).

The X-ray fiber diffraction patterns, and the corresponding equatorial profiles, of fibers stretched at various deformations of Figure 9, annealed at 110 °C for 20 min, keeping the fiber under tension, are reported in Figure 12. It is apparent that the fiber stretched at low deformation (100% strain), initially in the trans-planar form III (Figure 9A), transforms by annealing in a mixture of the antichiral helical form I and isochiral helical form II (Figure 12A). This is indicated by the strong increase of the intensity of the 200 reflection at $2\theta = 12°$ (common to forms I and II) and by the presence of the 020 reflection at $2\theta = 16°$ of form I and of the 110 reflection at $2\theta = 17°$ of form II in the diffraction pattern of Figure 12A,A′. It is worth mentioning that the transformation of the trans-planar form III into both helical forms I and II is a common behavior of s-PP and has been extensively described in the literature.[37,44]

The diffraction patterns of fibers stretched at higher values of deformation, initially in the form III (Figure 9B−D), after annealing (Figure 12B−D) still present reflections of the trans-planar form III (in particular the $(020)_t$, $(110)_t$, and $(130)_t$ at $2\theta = 16°$, 18°, and 30°, respectively, and the $(021)_t$, $(111)_t$ reflections on the first layer line) along with reflections of the helical forms I and II (200 reflection at $2\theta = 12°$, and the 020 and 110 reflections at $2\theta = 16°$ and 17° of forms I and II, respectively). The annealed fibers, stretched at 200−300% deformation, are therefore in mixtures of helical forms I and II and trans-planar form III (Figure 12B). In these annealed fibers the intensities of reflections of the trans-planar form III increase with increasing deformation, while the intensities of the reflections of the helical forms decrease (Figure 12C,D). For instance, in the diffraction pattern of the fiber stretched at 400% deformation and annealed (Figure 12C) the intensity of the peak at $2\theta = 16°$ becomes higher than that of the 200 reflection at $2\theta = 12°$ due to the contribution of the $(020)_t$ reflection of the form III. This indicates that when the fibers are stretched at high values of deformation ($\epsilon > 300\%$), the trans-planar form III obtained by stretching does not transform completely into the helical forms by annealing. With increasing deformation the amount of form III that transforms into the helical form by annealing decreases. Moreover, in the diffraction patterns of fibers stretched at high deformation and annealed (Figure 12D) the observed reflections of the helical forms are only at $2\theta = 12°$ and 16°, corresponding to the 200 and 020 reflections of the antichiral form I, whereas the 110 reflection at $2\theta = 17°$, typical of the helical form II, is no longer observed. This indicates that when the fibers are stretched at high strains the trans-planar form III transforms in part into the helical form I and not into the isochiral form II. A remarkable amount of crystals of the trans-planar form III, however, does not transform and remains stable even at high annealing temperature in fibers stretched at high deformation (Figure 12D).

These data indicate that in the sample sPP(PHI) the trans-planar form III obtained in stretched fibers is more stable than in the case of the metallocene-made s-PP. In the latter sample, indeed, the trans-planar form III is stable only under stretching and always transform

Table 3. Elastic Modulus (E), Stress (σ_b) and Strain (ϵ_b) at Break, Stress (σ_y) and Strain (ϵ_y) at the Yield Point, Tension Set at Break (t_b), and Crystallinity (x_c) of Unoriented Compression-Molded Films of the Samples sPP(PHI) and sPP(C_s)[a]

sample	[*rrrr*] %	M_w	E (MPa)	σ_b (MPa)	ϵ_b (%)	σ_y (MPa)	ϵ_y (%)	t_b (%)	x_c (%)[b]
sPP(PHI)	89.8	814 000	59 ± 6	20 ± 2	500 ± 20	12 ± 1	30 ± 1	132 ± 7	40
sPP(C_s)	91.0	164 000	295 ± 40	19 ± 1	580 ± 40	15 ± 1	25 ± 3	220 ± 10	45

[a] The fully syndiotactic pentad contents [*rrrr*] and the molecular weights (M_w) of the samples are also indicated. [b] From X-ray powder diffraction profiles.

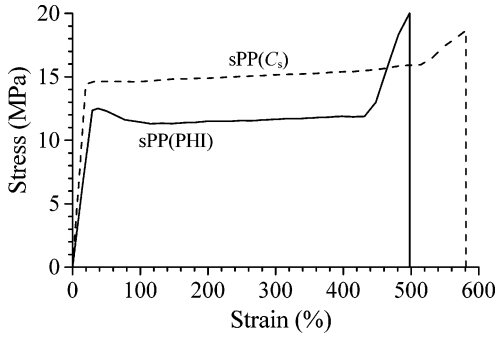

Figure 13. Stress−strain curves of unoriented compression-molded films of the sample sPP(PHI) (continuous line) compared to the stress−strain curve of a compression-molded film of the sample sPP(Cs) prepared with C_s-symmetric catalyst, taken from the ref 39 (dashed line).

in more stable modifications upon releasing the tension or by annealing.[39,40,44] In particular, the result that the trans-planar form III remains stable upon annealing has never been observed for metallocene-made s-PP. Moreover, it has been demonstrated that the structural evolution of the trans-planar form III upon removing the tension in stretched fibers strongly depends on the memory of the crystalline forms present in the starting unoriented material and of the crystalline forms produced during the stretching, so that form III always transforms into helical forms or in the trans-planar mesomorphic form when the fibers are relaxed.[55c]

The higher stability of the trans-planar form III for the sample sPP(PHI) is probably related to the microstructure, in particular the presence of nonnegligible amount (about 2%) of defects in the regular secondary (2,1) enchainment. As discussed above, the presence of (1,2) misinsertions produces formation of vicinal methylene carbon atoms $-CH_2-CH_2-$ along the polymer chains, which probably favors, locally, the formation of trans-planar sequences, which, in turn, may stabilize the trans-planar form III in stretched fibers.

Mechanical Properties. The stress−strain of the sample sPP(PHI) is reported in Figure 13 in comparison with the stress−strain curve of the sample sPP(Cs) from metallocene C_s-symmetric catalyst.[39] The values of the mechanical properties (Young's modulus, stress and strain at break, stress and strain at yield, and tension set) are reported in Table 3.

It is apparent that the main difference between mechanical properties of s-PP samples from the phenoxyimine catalyst of Chart 1 and from the C_s-symmetric metallocene catalyst is the lower value of the modulus of the sample sPP(PHI). This is probably due to presence of higher degrees of disorder in the crystals and the higher flexibility of chains induced by the presence of microstructural defects (*m* dyads and 1,2 misinsertions). Moreover, the lower value of the tension set after breaking of the sample sPP(PHI) (Table 3) indicates that this sample experiences a certain elastic recovery after breaking.

We recall that unoriented compression-molded films of highly stereoregular and crystalline s-PP samples from metallocene C_s catalysts do not show elastic behavior after the first stretching, as shown by the high value of tension set after breaking (t_b = 220%) reported in Table 3,[39] because the samples experience irreversible plastic deformation upon stretching (Figure 13). The crystalline domains, with chains in helical conformation, tend to assume a preferred orientation along the stretching direction originating a plastic, not reversible deformation.[39,48]

The stress−strain curves of Figure 13 indicate that also the compression-molded film of the sample sPP(PHI) experiences plastic deformation with yielding at high values of the stress, but most of the deformation is recovered, the residual deformation being only 132% after stretching up to 500% deformation (Table 3).

The mechanical analysis has also been performed on oriented stress-relaxed fibers, which generally present perfect elastic behavior in the case of s-PP samples from metallocene catalysts.[39,48] Stress-relaxed fibers have been prepared by stretching compression-molded films of the sample sPP(PHI) of initial length L_0 up to 500% elongation (the final length L_f being $6L_0$), keeping the fibers under tension for 10 min at room temperature and then removing the tension.

As discussed above and shown in Figure 11, stress-relaxed fibers are basically in the trans-planar mesomorphic form, in mixture with a small amount of crystals of the helical form I. The trans-planar form III, obtained by stretching at ϵ = 500% (Figure 11A), transforms, indeed, into the mesomorphic form and the helical form I by removing the tension (Figure 11B). The fibers present perfect elastic behavior upon successive stretching and relaxation mechanical cycles. The hysteresis cycles of the fibers, composed of the stress−strain curves measured during the stretching, immediately followed by the curves measured during the relaxation at controlled rate, are reported in Figure 14. In these cycles, stress-relaxed oriented fibers of the new initial length L_r are stretched up to the final length $L_f = 6L_0$.

Four successive cycles have been recorded; each cycle is performed 10 min after the end of the previous cycle. Successive hysteresis cycles, measured after the second one, are all nearly coincident, indicating a tension set close to zero. The stress-relaxed fibers recover almost completely the initial dimensions. The residual tension set between the first and second hysteresis cycles is around 10% and becomes close to zero starting from the second cycle, the successive cycles being all nearly coincident. These data indicate that oriented fibers present good elastic properties in a large range of deformation. The elastic recovery is associated with reversible polymorphic transitions between the trans-planar form III and the mesomorphic form, when the fiber are stretched at high deformations (Figure 11), or between the trans-planar form III and the helical form II, when the fibers are stretched at low degree of

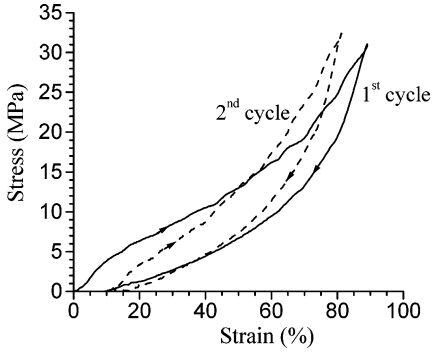

Figure 14. Stress−strain hysteresis cycles recorded at room temperature, composed of the stretching and relaxation (at controlled rate) steps according to the direction of the arrows, for strained and stress-relaxed fibers of the sample sPP(PHI). The fibers are prepared by stretching compression-molded films up to 500% elongation and then relaxed by removing the tension. In the hysteresis cycles the stretching steps are performed stretching the fibers up to the final length $L_f = 6L_0$. The first hysteresis cycle (continuous lines) and curves averaged for at least four cycles successive to the first one (dashed lines) are reported.

deformation (Figure 10), which occur in the crystals during the mechanical stress−relaxation cycles.

Conclusions

Analysis of the structure and the mechanical properties of syndiotactic polypropylene sample prepared with bis(phenoxyimine)titanium-based catalyst **2**/MAO of Chart 1 is reported. This catalyst belongs to a new family of nonmetallocene catalysts that are able to promote living polymerization of propylene, producing high molecular weight syndiotactic polypropylene.[20−22,30] The polymerization proceeds through a secondary (2,1) mechanism of enchainment of monomer and the syndiotactic stereoselectivity is due to the chain-end control.[20−22]

Because of the chain-end stereocontrol and the secondary (2,1) insertion chains of the resulting s-PP sample present a microstructure different from that of s-PP prepared with C_s-symmetric metallocene catalysts. They are indeed characterized by defects of stereoregularity represented basically by isolated *m* dyads (*..rrrmrrr..*), consistent with the chain-end mechanism, and vicinal methylene sequences as a result of occurrence of defects of regioregularity, due to primary (1,2) insertions in a prevailingly secondary (2,1) enchainment.[21,22] The effect of this different microstructure on the crystallization behavior and mechanical properties has been analyzed.

X-ray diffraction and solid-state ^{13}C NMR spectra have indicated that as-prepared samples crystallize in mixtures of crystals of helical form I and conformationally disordered modifications of the isochiral form II containing kink-bands. The formation of kink-bands modifications in the as-prepared sample is probably due to the presence of nonnegligible amount (about 2%) of defects in the regular secondary (2,1) enchainment, which produce vicinal methylene carbon atoms $-CH_2-CH_2-$. The presence of pairs of methylene groups along the polymer chains probably favors, locally, the formation of trans-planar sequences, which, in turn, induces the crystallization of the sample in the kink-bands disordered modification of form II.

These kink-bands disordered modifications are metastable and transform into the most stable antichiral helical form I by crystallization from the melt. However, disordered modifications of form I are obtained, even at high crystallization temperatures. In this sample the ordering in the alternation of right- and left-handed helical chains along both axes of unit cell, typical of the limit ordered form I, is prevented. Samples of s-PP of similar stereoregularity prepared with metallocene C_s-symmetric catalyst, instead crystallize from the melt at high crystallization temperature in the ordered form I, with a perfect alternation of right- and left-handed chains along the axes of the unit cell. The different behavior of the s-PP sample prepared with bis(phenoxyimine)titanium-based catalyst is probably due to the different microstructure and may be related to the presence of *m* dyads defects of stereoregularity, instead of *mm* triads defects. The presence of *m* defects may induce inversions of the helical chirality along s-PP chains. Since the macromolecular chains are very long (due to the very high molecular weight produced by the living polymerization) the occurrence of a not negligible amount of inversions is expected. As a consequence, correlations at long distances between the chiralities of the helices along *a* and *b* axes of the unit cell are destroyed. This produces departure from the fully antichiral packing of form I, introducing disorder in the regular alternation of right- and left-handed helical chains.

X-ray diffraction analysis of oriented fibers has demonstrated that the trans-planar form III obtained in stretched fibers does not transform completely in helical forms by releasing the tension or by annealing, as instead occurs in metallocene-made s-PP. This indicates that in the s-PP sample produced with the nonmetallocene catalyst the trans-planar form III is more stable than in the case of the metallocene-made s-PP. In the latter samples, indeed, the trans-planar form III is stable only under stretching and always transforms into more stable modifications upon releasing the tension or by annealing.[37,39,40,44]

The higher stability of the trans-planar form III for the nonmetallocene-made s-PP is probably related to the microstructure, in particular the presence of vicinal methylene carbon atoms $-CH_2-CH_2-$ along the polymer chains, due to (1,2) misinsertions, which probably favors, locally, the formation of trans-planar sequences, which, in turn, may stabilize the trans-planar form III in stretched fibers.

Analysis of the mechanical properties has shown that the s-PP sample from the nonmetallocene catalyst presents values of elastic modulus lower than that of highly stereoregular and crystalline metallocene-made s-PP. This is probably due to the presence of higher degrees of disorder in the crystals and the higher flexibility of chains induced by the presence of microstructural defects. Unoriented compression-molded samples show a remarkable elastic recovery even though the sample is crystalline and experiences plastic deformation during stretching. As a consequence, oriented fibers present good elastic properties, as for s-PP from metallocene catalysts, but in a larger deformation range. The elasticity is associated with polymorphic transitions occurring in the crystals during the mechanical stress−relaxation cycles.

Acknowledgment. Financial support from the "Ministero dell'Istruzione, dell'Università e della Ricerca" of Italy (PRIN 2002 and Cluster C26 projects) is gratefully

acknowledged. G.W.C. gratefully acknowledges support from the Packard, Beckman, and Sloan Foundations and the NSF (ECS-0103297). This research made use of the Cornell Center for Materials Research Shared Experimental Facilities supported through the NSF MRSEC program (DMR-0079992). The NMR polymer characterizations were carried out at Centro di Metodologie Chimico-Fisiche, University of Naples Federico II.

References and Notes

(1) Natta, G.; Zambelli, A.; Pasquon, P. *J. Am. Chem. Soc.* **1962**, *84*, 1488.
(2) Zambelli, A.; Locatelli, P.; Rovasoli, A.; Ferro, D. R. *Macromolecules* **1980**, *13*, 267.
(3) Ammendola, P.; Shijing, X.; Grassi, A.; Zambelli, A. *Gazz. Chim. Ital.* **1988**, *118*, 769.
(4) Zambelli, A.; Sessa, I.; Grisi, F.; Fusco, R.; Accomazzi, P. *Macromol. Rapid Commun.* **2001**, *22*, 297.
(5) Resconi, L.; Cavallo, L.; Fait, A.; Piemontesi, F. *Chem. Rev.* **2000**, *100*, 1253.
(6) Resconi, L.; Camurati, I.; Sudmeijer, O. *Top. Catal.* **1999**, *7*, 145.
(7) Spaleck, W.; Antberg, M.; Aulbach, M.; Bachmann, B.; Dolle, V.; Haftka, S.; Küber, F.; Rohrmann, J.; Winter, A. In *Ziegler Catalysts*; Fink, G., Mülhaupt, R., Brintzinger, H. H., Eds.; Springer-Verlag: Berlin, 1995; pp 84−97.
(8) Resconi, L.; Moscardi, G. *Polym. Prepr.* (*Am. Chem. Soc., Div. Polym. Chem.*) **1997**, *38*, 832.
(9) Miyatake, T.; Mizunuma, K.; Kakugo, M. *Makromol. Chem., Macromol. Symp.* **1993**, *66*, 203.
(10) Small, B. L.; Brookhart, M.; Bennett, A. M. A. *J. Am. Chem. Soc.* **1998**, *120*, 4049.
(11) Britovsek, G. J. P.; Gibson, V. C.; Kimberley, B. S.; Maddox, P. J.; McTavish, S. J.; Solan, G. A.; White, A. J. P.; Williams, D. J. *Chem. Commun.* **1998**, 849.
(12) Small, B. L.; Brookhart, M. *Polym. Prepr.* (*Am. Chem. Soc., Div. Polym. Chem.*) **1998**, *39*, 213.
(13) Pellecchia, C.; Mazzeo, M.; Pappalardo, D. *Macromol. Rapid Commun.* **1998**, *19*, 651.
(14) Small, B. L.; Brookhart, M. *Macromolecules* **1999**, *32*, 2120.
(15) Ewen, J. A. *J. Am. Chem. Soc.* **1984**, *106*, 6355.
(16) Pellecchia, C.; Zambelli, A. *Makromol. Chem., Rapid Commun.* **1996**, *17*, 333.
(17) Pellecchia, C.; Zambelli, A.; Oliva, L.; Pappalardo, D. *Macromolecules* **1996**, *29*, 6990.
(18) Pellecchia, C.; Zambelli, A.; Mazzeo, M.; Pappalardo, D. *J. Mol. Catal. A: Chem.* **1998**, *128*, 229.
(19) McCord, E. F.; McLain, S. J.; Nelson, L. T. J.; Arthur, S. D.; Coughlin, E. B.; Ittel, S. D.; Johnson, L. K.; Tempel, D.; Killian, C. M.; Brookhart, M. *Macromolecules* **2001**, *34*, 362.
(20) Tian, J.; Coates, G. W. *Angew. Chem., Int. Ed.* **2000**, *39*, 3626.
(21) Tian, J.; Hustad, P. D.; Coates, G. W. *J. Am. Chem. Soc.* **2001**, *123*, 5134.
(22) Hustad, P. D.; Tian, J.; Coates, G. W. *J. Am. Chem. Soc.* **2002**, *124*, 3614.
(23) Matsui, S.; Mitani, M.; Saito, J.; Tohi, Y.; Makio, H.; Tanaka, H.; Fujita, T. *Chem. Lett.* **1999**, 1263. Matsui, S.; Tohi, Y.; Mitani, M.; Saito, J.; Makio, H.; Tanaka, H.; Nitabaru, M.; Nakano, T.; Fujita, T. *Chem. Lett.* **1999**, 1065. Matsui, S.; Mitani, M.; Saito, J.; Matsukawa, N.; Tanaka, H.; Nakano, T.; Fujita, T. *Chem. Lett.* **2000**, 554.
(24) Matsui, S.; Mitani, M.; Saito, J.; Tohi, Y.; Makio, H.; Matsukawa, N.; Takagi, Y.; Tsuru, K.; Nitabaru, M.; Nakano, T.; Tanaka, H.; Kashiwa, N.; Fujita, T. *J. Am. Chem. Soc.* **2001**, *123*, 6847.
(25) Matsui, S.; Fujita, T. *Catal. Today* **2001**, *66*, 63.
(26) Matsui, S.; Inoue, Y.; Fujita, T. *J. Synth. Org. Chem. Jpn.* **2001**, *59*, 232.
(27) Matsukawa, N.; Matsui, S.; Mitani, M.; Saito, J.; Tsuru, K.; Kashiwa, N.; Fujita, T. *J. Mol. Catal. A: Chem.* **2001**, *169*, 99.
(28) Saito, J.; Mitani, M.; Mohri, J.; Yoshida, Y.; Matsui, S.; Ishii, S.; Kojoh, S.; Kashiwa, N.; Fujita, T. *Angew. Chem., Int. Ed.* **2001**, *40*, 2918.
(29) Kaminsky, W.; Kulper, K.; Brintzinger, H. H.; Wild, F. *Angew. Chem., Int. Ed. Engl.* **1985**, *24*, 507.
(30) Saito, J.; Mitani, M.; Onda, M.; Mohri, J. I.; Ishii, S. I.; Yoshida, Y.; Nakano, T.; Tanaka, H.; Matsugi, T.; Kojoh, S. I.; Kashiwa, N.; Fujita, T. *Macromol. Rapid Commun.* **2001**, *22*, 1072.
(31) Ewen, J. A.; Jones, R. J.; Razavi, A.; Ferrara, J. D. *J. Am. Chem. Soc.* **1988**, *110*, 6255.
(32) De Rosa, C.; Auriemma, F.; Circelli, T.; Waymouth, R. M. *Macromolecules* **2002**, *35*, 3622.
(33) Auriemma, F.; De Rosa, C. *Macromolecules* **2002**, *35*, 9057.
(34) De Rosa, C.; Auriemma, F.; Spera, C.; Talarico, G.; Tarallo, O. *Macromolecules* **2004**, *37*, 1441.
(35) De Rosa, C.; Auriemma, F.; Perretta, C. *Macromolecules* **2004**, *37*, 6843.
(36) De Rosa, C.; Auriemma, F.; Vinti, V. *Macromolecules* **1997**, *30*, 4137.
(37) De Rosa, C.; Auriemma, F.; Vinti, V. *Macromolecules* **1998**, *31*, 7430.
(38) De Rosa, C.; Auriemma, F.; Vinti, V.; Galimberti, M. *Macromolecules* **1998**, *31*, 6206.
(39) Auriemma, F.; Ruiz de Ballesteros, O.; De Rosa, C. *Macromolecules* **2001**, *34*, 4485.
(40) Auriemma, F.; De Rosa, C. *J. Am. Chem. Soc.* **2003**, *125,* 13144. *Macromolecules* **2003**, *36*, 9396.
(41) Lotz, B.; Lovinger, A. J.; Cais, R. E. *Macromolecules* **1988**, *21*, 2375. Lovinger, A. J.; Lotz, B.; Davis, D. D. *Polymer* **1990**, *31*, 2253. Lovinger, A. J.; Davis, D. D.; Lotz, B. *Macromolecules* **1991**, *24*, 552. Lovinger, A. J.; Lotz, B.; Davis, D. D.; Padden, F. J. *Macromolecules* **1993**, *26*, 3494.
(42) Chatani, Y.; Maruyama, H.; Noguchi, K.; Asanuma, T.; Shiomura, T. *J. Polym. Sci., Part C* **1990**, *28*, 393.
(43) Chatani, Y.; Maruyama, H.; Asanuma, T.; Shiomura, T. *J. Polym. Sci., Polym. Phys.* **1991**, *29*, 1649.
(44) De Rosa, C.; Corradini, P. *Macromolecules* **1993**, *26*, 5711.
(45) Auriemma, C.; De Rosa, C.; Corradini, P. *Macromolecules* **1993**, *26*, 5719.
(46) De Rosa, C.; Auriemma, F.; Corradini, P. *Macromolecules* **1996**, *29*, 7452.
(47) Auriemma, F.; De Rosa, C.; Ruiz de Ballesteros, O.; Vinti, V. *J. Polym. Sci., Polym. Phys.* **1998**, *36*, 395.
(48) De Rosa, C.; Gargiulo, M. C.; Auriemma, F.; Ruiz de Ballesteros, O.; Razavi, A. *Macromolecules* **2002**, *35*, 9083.
(49) De Rosa, C.; Auriemma, F.; Ruiz de Ballesteros, O.; Resconi, L.; Fait, A.; Ciaccia, E.; Camurati, I. *J. Am. Chem. Soc.* **2003**, *125*, 10913.
(50) De Rosa, C.; Auriemma, F.; Ruiz de Ballesteros, O. *Macromolecules* **2003**, *36*, 7607.
(51) De Rosa, C.; Auriemma, F.; Ruiz de Ballesteros, O. *Macromolecules* **2004**, *37*, 1422.
(52) Resconi, L.; Guidotti, S.; Baruzzi, G.; Grandini, C.; Nifant'ev, I. E.; Kashulin, I. A.; Ivchenko, P. V. PCT Int. Appl. WO 01/53360, 2001, Basell, Italy. Grandini, C.; Camurati, I.; Guidotti, S.; Mascellari, N.; Resconi, L.; Nifant'ev, I. E.; Kashulin, I. A.; Ivchenko, P. V.; Mercandelli, P.; Sironi, A. *Organometallics* **2004**, *23*, 344.
(53) Nakaoki, T.; Ohira, Y.; Hayashi, H.; Horii, F. *Macromolecules* **1998**, *31*, 2705.
(54) Vittoria, V.; Guadagno, L.; Comotti, A.; Simonutti, R.; Auriemma, F.; De Rosa, C. *Macromolecules* **2000**, *33*, 6200.
(55) (a) De Rosa, C.; Auriemma, F.; Ruiz de Ballesteros, O. *Polymer* **2001**, *42*, 9729. (b) De Rosa, C.; Ruiz de Ballesteros, O.; Santoro, M.; Auriemma, F. *Polymer* **2003**, *44*, 6267. (c) De Rosa, C.; Ruiz de Ballesteros, O.; Santoro, M.; Auriemma, F. *Macromolecules* **2004**, *37*, 1816. (d) **2004**, *37*, 7724.
(56) Corradini, P.; Natta, G.; Ganis, P.; Temussi, P. A. *J. Polym. Sci., Part C* **1967**, *16*, 2477.
(57) Loos, J.; Hückert, A.; Petermann, J. *Colloid Polym. Sci.* **1996**, *274*, 1006. Loos, J.; Petermann, J.; Waldöfner, A. *Colloid Polym. Sci.* **1997**, *275*, 1088.
(58) Grassi, A.; Zambelli, A.; Resconi, L.; Albizzati, E.; Mazzocchi, R. *Macromolecules* **1988**, *21*, 617. Zambelli, A.; Gatti, G. *Macromolecules* **1978**, *11*, 485.
(59) Auriemma, F.; Born, R.; Spiess, H. W.; De Rosa, C.; Corradini, P. *Macromolecules* **1995**, *28*, 6902. Auriemma, F.; Lewis, R. H.; Spiess, H. W.; De Rosa, C. *Macromol. Chem. Phys.* **1995**, *196*, 4011. Auriemma, F.; De Rosa, C.; Ruiz de Ballesteros, O.; Corradini, P. *Macromolecules* **1997**, *30*, 6586.
(60) Bunn, A.; Cudby, E. A.; Harris, R. K.; Packer, K. J.; Say, B. J. *J. Chem. Soc., Chem. Commun.* **1981**, 15. Sozzani, P.; Simonutti, R.; Galimberti, M. *Macromolecules* **1993**, *26*, 5782.
(61) Sozzani, P.; Galimberti, M.; Balbontin, G. *Makromol. Chem. Rapid Commun.* **1993**, *13*, 305.
(62) De Rosa, C.; Auriemma, F.; Vinti, V.; Grassi, A.; Galimberti, M. *Polymer* **1998**, *39*, 6219. De Rosa, C.; Auriemma, F.; Talarico, G.; Busico, V.; Caporaso, L.; Capitani, D. *Macromolecules* **2001**, *35*, 1314. De Rosa, C.; Auriemma, F.; Fanelli, E.; Talarico, G.; Capitani, D. *Macromolecules* **2003**, *36*, 1850.

MA048753J